JEE Journal of Ecological Engineering

Journal of Ecological Engineering, 2026, 27(2), 388–400
https://doi.org/10.12911/22998993/211688
ISSN 2299–8993, License CC-BY 4.0

Received: 2025.08.11
Accepted: 2025.12.15
Published: 2026.01.15

Assessment of air quality in the urban environment taking into account vegetation and building geometry

Perizat Omarova[1], Tong Yang[2], Aisulu Ataniyazova[1], Ainur Kozbakova[1*], Didar Yedilkhan[3]

[1] Institute of Information and Computational Technologies CS MSHE RK, Al-Farabi Kazakh National University, 28 Shevchenko str., Almaty, Kazakhstan
[2] Faculty of Science and Technology, Middlesex University, London, United Kingdom
[3] Smart City Research and Innovation Center, Astana IT University, Astana, Kazakhstan
* Corresponding author's e-mail: ajnurkozbakova@gmail.com

ABSTRACT

In this paper, the influence of a perpendicular structure in front of parallel buildings on the stabilization of pollutants is investigated, taking into account the porous medium. And to test the model, numerical simulation was carried out formulated using the Navier-Stokes governing equations. It is worth noting that attention is paid to configurations with a perpendicularly located box, in the middle of which there is a porous barrier simulating trees. Thus, this allows more realistically reproducing the conditions of the urban environment. The study is based on a test problem reproducing experimental conditions and the use of the RNG k–ε turbulent model. Simulation showed that the presence of perpendicular structures significantly affects the movement of air flows and the distribution of pollutant concentrations. Model adjustments for turbulent viscosity in critical areas were changed with the aim of improving forecast precision of impurity transport. Analysis of the vertical profile of concentrations revealed critical zones where harmful substances accumulate, especially at the level of y/H = 1.26. The results were evaluated with experimental data and confirm the reliability of the numerical approach. Also, the distribution of concentration by height changes sharply and at the base of the wall (y/H = 0) it decreases to 0.4, and at y/H = 1.26 it reaches a maximum showing a high level of pollution. The obtained results are relevant for the environmental analysis of the urban environment and can be used in planning measures to improve air quality. In the future, it is planned to expand the modeling to more complex urban areas taking into account the relief, multiple sources of pollution and weather conditions, which will improve the accuracy of forecasts and the effectiveness of environmental regulation.

Keywords: air quality, numerical simulation, porous media, street canyons.

INTRODUCTION

Air pollution has become a pressing issue in Almaty, Kazakhstan, due to rapid urbanization, increased vehicular emissions, and industrial activities (Kerimray et al., 2020a). The city's geographical location in a valley surrounded by mountains exacerbates the accumulation of pollutants, particularly during winter when temperature inversions trap emissions near the surface (Kerimray et al., 2020b), (Kerimray et al., 2020c). High amounts of particulate pollutants (PM2.5 and PM10) accompanied by substantial nitrogen dioxide (NO_2) and sulfur dioxide (SO_2) level pose serious health risks to residents, making air quality management a crucial challenge (Assanov al., 2021).

Vegetation alters urban microclimate by deposition (leaves adsorb/absorb pollutants) and aerodynamics (trees act as porous obstacles) (Yang et al., 2020). Reviews emphasize this trade-off: trees can reduce pollutants by leaf deposition, but also impede airflow and intensify canyon trapping (Wang et al., 2020). The researchers noted in their work (Barwise et al., 2020) that the design of green barriers should provide a balance between

improved precipitation and reduced ventilation. For instance, explicit CFD simulations with detailed tree models show that tree canopies slow wind and shift recirculation zones: low-velocity pockets form around tree crowns, especially at pedestrian height, causing persistent pollutant hotspots on the leeward canyon side (Wang et al., 2020). In one study, obstacles like foliage created dynamic pollutant patches at the bottom of the canyon, illustrating how canopy-induced vortices trap emissions. Similarly, research (B´zdziuch et al., 2024) compared real-world canyon data and found that adding dense roadside vegetation could raise near-ground concentrations.

Despite potential drawbacks for dispersion, vegetation still provides net benefits through pollutant deposition. Using CFD separated aerodynamic from dry-deposition effects in Seoul and showed that while tree canopies slightly increased on-road NOx due to flow obstruction, deposition reduced sidewalk NOx enough to yield an overall decrease (Kim et al., 2025). These effects vary with wind speed and leaf surface properties, underscoring that species and placement must maximize deposition while minimizing flow blockage. (Badach et al., 2020) likewise recommend species with small, hairy or waxy leaves to enhance PM capture, noting that standard deposition rates may not reflect local climates or fine particles.

Microscale CFD studies illustrate these principles. (Liu and Zheng, 2023) found that moderate spacing of shorter trees improved PM2.5 dispersion, whereas dense tall trees hindered it; (Wang et al., 2020) also showed that realistic tree geometries reduce airflow and reshape vortex patterns. Overall, sparse or shorter vegetation tends to benefit dispersion, while dense, tall canopies trap pollutants near ground level.

Roadside barrier research confirms this dual role. (Santiago et al., 2019) reported that tree–hedge combinations reduced black carbon concentrations by up to 66% at 15 m downwind compared with no barrier. Jeong et al. (2023) and Deng et al. (2018) found that multi-layer plantings combining taller trees with lower shrubs achieved the lowest PM2.5 concentrations. These results demonstrate that green infrastructure can capture pollutants if configured appropriately (height, density, species, layering), but knowledge gaps remain about local deposition rates, seasonal effects and the net health impact of partial reductions.

Modern machine learning and deep learning methods are increasingly used to forecast urban air pollution from heterogeneous meteorological and traffic data. Models such as Random Forest, Gradient Boosting and hybrid physics-informed approaches improve short-term predictions and complement CFD by enabling rapid scenario analysis (Zhang et al., 2020). Moreover, for large cities with intensive development and complex air ventilation systems, neural networks such as LSTM and ConvLSTM are effectively used to analyze spatial dependencies in pollutant data (Li et al., 2022; Yedilkhan et al., 2025; Altaibek et al., 2024). In addition, the implementation of ML/DL models with physical-mathematical equations of pollutant transport based on the Navier-Stokes and diffusion equations shows an advantage for hybrid modeling (Physics-Informed Neural Networks, PINNs), which takes into account empirical data and physical laws (Raissi et al., 2019; Omarova et al., 2023; Kalesh et al., 2025a; Kalesh et al., 2025b; Baydaulet et al., 2024). This approach provides more accurate and reliable forecasts are presented, which helps with effective decision-making in the field of air quality management.

The layout of the building profoundly influences urban ventilation. The aspect ratio of the street canyon (building height H to street width W) is a key parameter: low H/W (short buildings or a wide street) generally allows better dispersion, while deep canyons trap pollutants. In the context of this study, for example (Buccolieri et al., 2021) found H/W=2 was critical: deeper canyons dramatically enhance horizontal pollutant accumulation at pedestrian level.

Practical guidelines typically recommend maintaining an aspect ratio H/W<1 to minimize airflow stagnation within street canyons (Oke, 2002). In contrast, architectural modifications, such as introducing large openings or void spaces in building designs, can significantly enhance ventilation. For instance, Sin et al. (2023) used CFD simulations in asymmetric street canyons and demonstrated that incorporating a "void deck" a ground – level opening – considerably increased air exchange. Their findings indicated that implementing a 3 meter high void increased air exchange rates by approximately 148–416 and substantially reduced pollutant concentrations along the adjacent building facade.

Larger void decks (4.5 m) provided even stronger ventilation gains, raising air change rates

by 177–381. Similarly Li, D. et al. (2022) showed that urban blocks with open plazas and tall towers improved airflow – open courtyards increased wind speed by 0.4–2.3 m/s, while a central 2×H high-rise boosted it by up to 23%, lowering CO levels by 4–23% and reducing intake fractions by ~24%. Such findings imply that lifting first floors or adding plazas can effectively redirect winds. Elevated buildings are especially promising: ground-level voids reduced street pollution by 30–50% compared to solid foundations, with the strongest effect from full elevation (Buccolieri et al., 2021; Sha et al., 2018). Overall, building permeability – via stilted or cut-through structures, wider street axes, or permeable facades – markedly improves ventilation.

Most recent research uses CFD (Reynolds-Averaged Navier-Stokes) and LES (Large Eddy Simulation) models dominate, often with boundary-layer wind profiles. For instance, Wang et al. (2020) explicitly solved the Navier-Stokes equations to simulate airflow dynamics within street canyons. Such simulations reveal how variations in building and vegetation geometry affect vortex structures and pollutant dispersion, and systematic reviews highlight the need for 3D models for accuracy (Pantusheva et al., 2022). Model credibility, however, still depends on validation with field or wind-tunnel data, as shown by Bzdziuch et al. (2024). Observational campaigns on vegetation impacts remain scarce and yield mixed results due to seasonal foliage and meteorological effects; reviews indicate that core factors such as geometry and inflow dominate over secondary influences (Zhang et al., 2020). Combined approaches - sensor networks calibrated by CFD and multi-scale, ML-enhanced frameworks - are now emerging (Pantusheva et al., 2022).

In megacities of Asia and Central Asia, including winter-inverted Almaty, effective air-quality measures require avoiding overly tall and dense plantings and designing wider or permeable corridors. Architectural innovations such as open ground floors and interior plazas, supported by studies like Sin et al. (2023) and Buccolieri et al. (2021), can markedly enhance ventilation but must be tested under local conditions. Knowledge gaps include leaf-off deposition rates, pollutant chemistry and large-domain LES or coupled meso-micro modeling to capture city-scale flows.

Overall, recent studies (2018–2024) show that vegetation can significantly remove pollutants but often at the cost of airflow, creating trade-offs that must be carefully managed. Our work contributes to this body of knowledge by numerically modeling a novel perpendicular box configuration with porous barriers to clarify how urban form reshapes pollutant dispersion, providing a basis for more targeted urban-air-quality strategies.

Indoor air pollution modeling has also used the Navier-Stokes equations, particularly to study ventilation efficiency and pollutant distribution in enclosed spaces (Mutlu, 2020; Mohammadi et al., 2021). These studies highlight the role of airflow patterns and HVAC (heating, ventilation, and air conditioning) systems in mitigating indoor air contamination. The advantage of this approach lies in its ability to provide detailed insights into pollutant dynamics, although the high computational demand remains a limit.

METHODOLOGY

The mathematical model

The mathematical formulation of the problem in this work was performed in the ANSYS Fluent 2020 R1 environment (Theory Guide; User's Guide, Canonsburg, PA, USA, 2020). To determine the velocity field and concentration distribution, the time averaged equations of conservation of mass, momentum, and scalar transfer are used:

$$\frac{\partial u_i}{\partial x_i} = 0 \tag{1}$$

$$\frac{\partial u_i}{\partial t} + \frac{\partial(\rho u_i u_j)}{\partial x_j} = \frac{\partial\left(-\rho\overline{u_i' u_j'}\right)}{\partial x} - \\ -\frac{\partial P}{\partial x_i} + \frac{\partial}{\partial x_j}\left(\mu\left(\frac{\partial u_i}{\partial x_j} + \frac{\partial u_j}{\partial x_i}\right)\right) \tag{2}$$

$$\frac{\partial C}{\partial t} + \frac{\partial \rho u_i C}{\partial x_j} = \frac{\partial\left(-\rho\overline{u_j' C'}\right)}{\partial x_j} - \\ -\frac{\partial}{\partial x_j} + \left(\gamma\frac{\partial C}{\partial x_j}\right) \tag{3}$$

where: μ_i – speed, ρ – liquid density, P – fluid pressure, C – concentration, γ – molecular diffusion coefficient, μ – dynamic viscosity, $\overline{u_i' u_j'}$ and $\overline{u_j' C'}$ – Reynolds-averaged velocities and stress concentration flows.

The turbulent models

Turbulent models were used for this study $k-\varepsilon$. Standard and $k-\varepsilon$ RNG.

Turbulent model $k-\varepsilon$

$$\frac{\partial k}{\partial t}+\frac{\partial}{\partial x_j}(u_j k)=\frac{\partial}{\partial x_j}\left[\left(\mu+\frac{\mu_t}{\sigma_k}\right)\frac{\partial k}{\partial x_j}\right]+ +P_k+\rho\varepsilon+P_{kb} \quad (4)$$

$$\frac{\partial \varepsilon}{\partial t}+\frac{\partial}{\partial x_j}(u_j \varepsilon)=\frac{\partial}{\partial x_j}\left[\left(\mu+\frac{\mu_t}{\sigma_\varepsilon}\right)\frac{\partial \varepsilon}{\partial x_j}\right]+ +\frac{\varepsilon}{k}(C_{\varepsilon 1}P_k-C_{\varepsilon 2}\rho\varepsilon+C_{\varepsilon 3}P_{kb}) \quad (5)$$

Here k – turbulent kinetic energy, ε – turbulent dissipation, P_k – formation of turbulence due to viscous forces:

$$P_k=\mu_t\left(\frac{\partial u_i}{\partial x_j}+\frac{\partial u_j}{\partial x_j}\right)\frac{\partial u_i}{\partial x_j}- -\frac{2}{3}\frac{\partial u_k}{\partial x_k}\left(3\mu_t+\frac{\partial u_t}{\partial x_k}+\rho k\right) \quad (6)$$

where: $P_k=-\frac{\mu_t}{\sigma_\rho}\beta g_i\frac{\partial T}{x_i}$ and

$P_{\varepsilon b}$ = $C_3(0, p_{KB})$ – represent buoyancy forces. Here β – coefficient of thermal expansion, $\sigma_\rho = 0.9$, $C\mu = 0.09$, $C_{\varepsilon 1}$, $C_{\varepsilon 2\rho}$, σ_ε, σ_k – permanent.

Numerical simulation algorithm

To obtain the pressure and velocity fields in an incompressible medium, the SIMPLE method (Semi-Implicit Method for Pressure-Linked Equations) is used. In general terms, the procedure is reduced to the following sequence of steps:

1. Representations of the initial pressure P^0 and give fields $P^*=P^0$, t=0
2. Definitions of the initial velocity field u^0, v^0.
3. Solving the momentum equations for obtaining u^*, v^*.
4. Solving the equation for P′and calculating P by adding P′to P^*.
5. Finding u, v by means of formulas for velocity correction.
6. In the case $|P'|$ that there is little in all nodes of the computational grid, then we assume $P^0=P$, $u^0=u$, $v^0=v$, t = t + Δt. Otherwise, it uses what was found Plike $P^*$and go to step 3.
7. If, $t<T_{max}$ then we have to return the step 3.

RESULTS

Test problem

To assess the dispersion of pollutants in a street canyon with a porous barrier, a test was performed using a similar model developed by (Salim et al., 2011a; Salim et al., 2011b). In an experiment conducted at the Karlsruhe Institute of Technology, a porous tree crown was used as a barrier to simulate urban vegetation. The study used an idealized three-dimensional street canyon in the center with two symmetrical buildings (H = 18 m, L = 180 m, W = 18 m) and a porous barrier (9 × 180 × 12 m), and the distance of the porous barrier from the building is 4.5 m with a side. The estimated area was 540 × 432 × 144 m. The dispersion of pollutants was analyzed using sulfur hexafluoride (Sf_6) as an indicator gas, which was released along the longitudinal axis at a distance of 4.5 m from the canyon wall at ground level and 1.6 m wide, and the Q emission level increased by 10 g/l. The results were verified and compared with experimental data from (Salim et al., 2011a), who studied the dispersion of pollutants in a street canyon with a porous barrier. Thus, considering various canyons, the proven numerical model using the k–ε RNG turbulence model helps improve the numerical modeling of air pollution in urban conditions. The full size of the area under study and the boundary conditions are shown in Figure 1. In this paper, trees were modeled as porous barriers with a height of 12 meters, a width of 9 meters, and a length of 180 meters, which helps to more realistically simulate the spread of pollutants in the urban environment, taking into account trees. For the crown of trees, porosity was determined based on experimental data as follows (Salim et al., 2011a):

$$P_{vol} = 97.5\%,\ \lambda = 80\ m^{-1} \quad (7)$$

$$P_{vol} = 96\%,\ \lambda = 200\ m^{-1} \quad (8)$$

The RNG model k–ε was chosen to solve the Reynolds-averaged Navier-Stokes equations (RANS) because it accurately predicts the average flow characteristics and large-scale vortices under challenging conditions. Previous studies by Tominaga (2015) and Wijesooriya et al. (2023) have confirmed its effectiveness in modeling periodic fluctuations and the distribution of flows around buildings. The model reduces the overproduction of turbulent kinetic energy (TCE) in flow collision zones, which improves

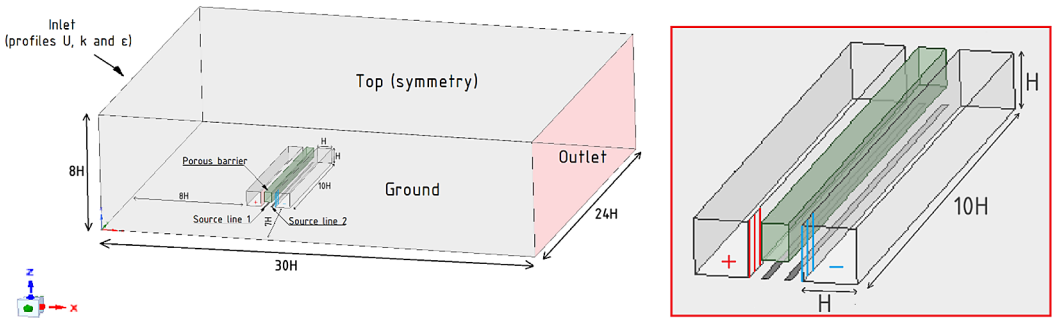

Figure 1. Computational domain model for the test problem, H = 18 m

the prediction of air flows and helps reduce pollution. In this study, URANS calculations using the *k–ε* RNG model with a modified ε equation showed the best agreement with experimental data. Moreover, thickening was set in certain areas to obtain more accurate simulation results.

Therefore, the use of a fine grid, taking into account the local characteristics of the current, helps to reduce computational calculations and was set as follows: source line – 0.45 meters, inlet – 1.5 meters, canyons – 0.65 meters, canyons – 2.5 meters, box – 4 meters. The thickening of the grid in certain areas in the boundary layer plays an important role in more accurate RANS modeling. In the works of Weaver et. al. (2021) showed the importance of adjusting models of turbulent viscosity in RANS modeling as it improves the prediction of scalar transport and turbulent flows of complex geometry. Therefore, this study carried out condensation in certain areas as an unstructured grid to obtain more accurate results. The computational area downstream of the barrier contained 592,831 elements in total, including 102,985 nodes. It is worth noting that special attention was paid to the boundary layer when building the grid. The general view of the calculated grid is shown in Figure 2.

User-defined functions were applied to evaluate the consistency of numerical simulation results with user-defined experimental data (UDF). The inlet velocity profile is imposed as a boundary condition and is mostly maintained, except in regions with flow detachment and turbulence around obstructions. As we can see, the numerical simulation results agree with the experimental data, and the velocity profile is shown in Figure 3. The side wind is determined using a custom detection function according to experimental data by (Salim et al., 2011a).

$$u(z) = 4.7\left(\frac{z}{0.12}\right)^{0.3}\frac{m}{s} \tag{9}$$

Figure 4 illustrates the coordinates of the lines along which the numerical simulation results. The measurements were carried out on six control lines distributed along both walls of the street canyon (three lines on each wall (wall A "red +" and wall B "blue –"): y/H = 0, y/H = 1.26 and y/H = 3.79). It is important to note that the locations of the control lines were carefully selected based on the geometry of the object being studied, which helps to describe the results of numerical modeling. Coordinates of the lines at Sf_6 Molar concentration Wall A/B. Figure 3 shows the vertical profiles of the air velocity at the inlet of the study area and the normalized height along the X-axis. The results obtained are assessed in relation to the experimental results (circles), numerical results (black line) and the simulation data according to (Salim et al., 2011a; Salim et al., 2011b) (red line), which are in good agreement with each other.

Sulfur hexafluoride (Sf_6) was chosen as a pollutant because of its unique characteristics and ease of measurement. Moreover, this approach is based on the reliability of obtaining data on concentrations of contaminants in the atmosphere and the availability of technologies for their accurate measurement, which helps to get precise results when studying the effects of pollutants in street canyons, where a correct and stable measuring base is required. We received the concentration profile in six control lines based on the control lines shown in Figure 4. The results can be observed in Figure 5. As we can see, the concentration distribution of the LES model corresponds significantly better along wall A, and the RSM model shows a significant improvement in results along wall B. The numerical simulation results are much better and agree with the experimental data. In addition, various numerical methods

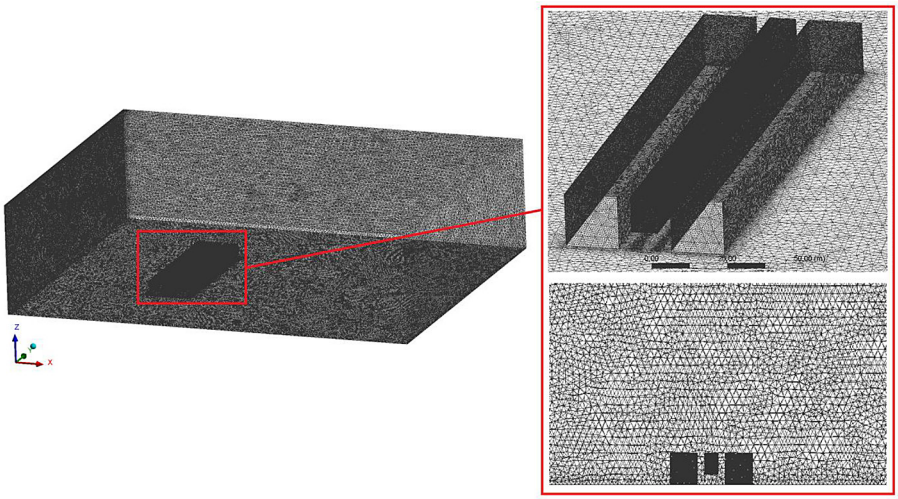

Figure 2. Computational grid

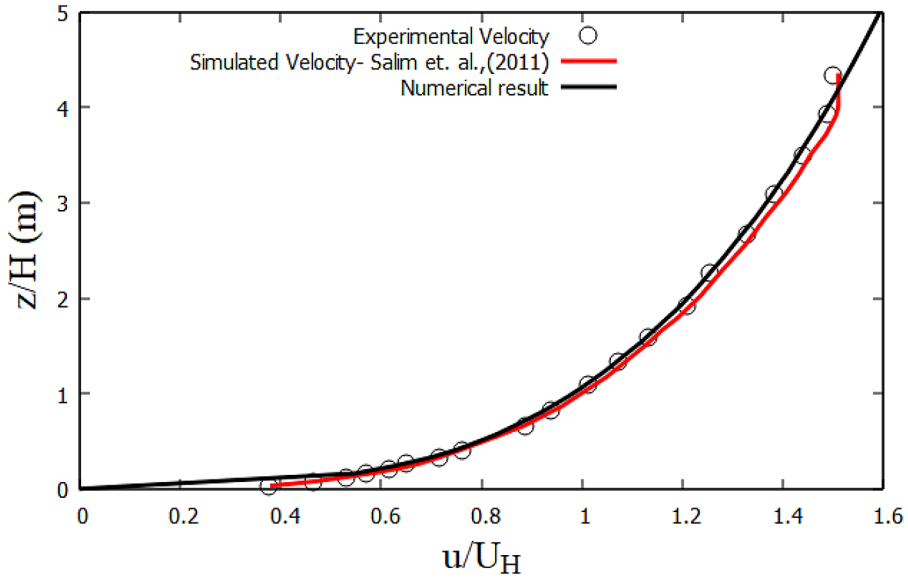

Figure 3. The velocity profile

compared forecasts (Salim et al., 2011a; Salim et al., 2011b) based on average normalized values and concentration contours along the mean plane y/H = 0 inside canyon street

Based on the results obtained, we draw the following conclusions: the chosen numerical model can be applied to describe cases with expanded geometry and a porous barrier. Also, the results of the cross-sectional contour for velocity and molar concentration of Sf_6 are shown in Figure 6. It also shows the coordinates Y = 125.65 (Plane 1), Y = 185.65 (Plane 2), Y = 235.65 (Plane 3), Y = 285.65 (Plane 4). As shown, the measurement plane was located along the Z-width. Notably, the variation in speed is observed in the middle of the wind tunnel, where the perpendicular positioning of the canyon alters the speed and creates small vortices. And the change in velocity along the porous barrier can only be seen in plane 1, since it is located close to the side wall, as well as the influence of incoming wind. It is also worth noting that the change in the molar concentration of Sf_6 along the walls increases with the accumulation of maximum concentration. As a result, significant dynamics of concentration changes are observed in this area.

The two-dimensional and three-dimensional distribution of the molar concentration of Sf_6 is shown in Figure 7. This figure demonstrates the

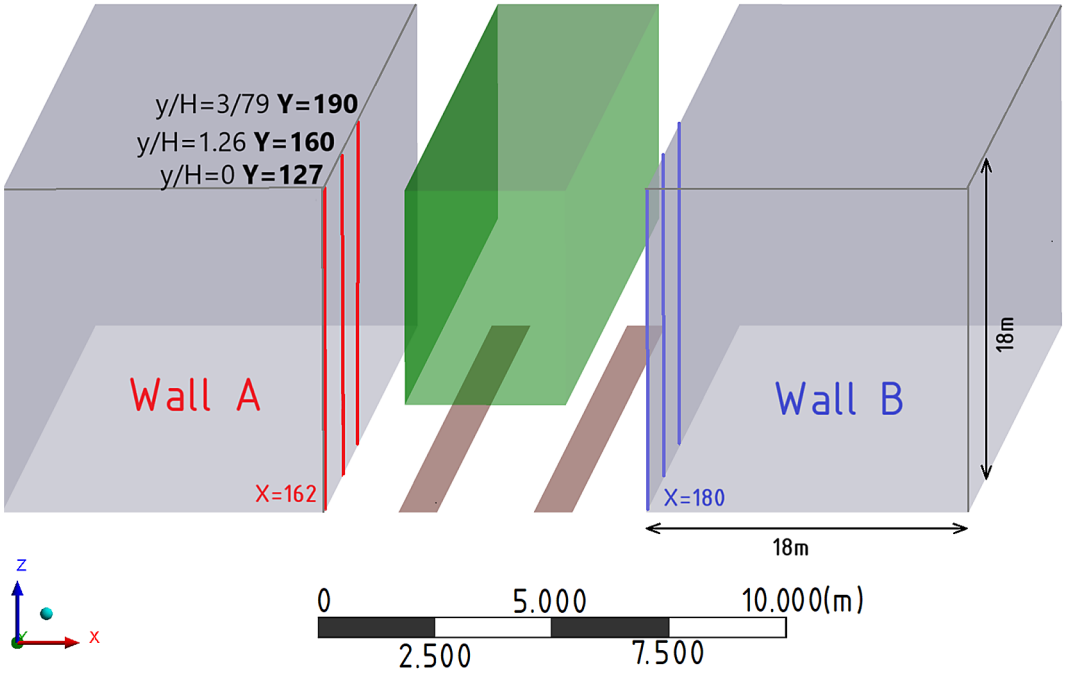

Figure 4. Location of control line

impact of the porous barrier on the concentration distribution within the canyons.

Moreover, the concentration spreads vertically along the Y wall, creating air circulation inside the canyon. Despite this, the concentration accumulates much higher in the middle of the canyon along the Y-axis than in the initial and final parts of the canyon. This can be explained by the fact that the length and height of the boxes play an important role in the flow rate, and there is an accumulation of concentricity due to a decrease in wind speed. Thus, the presence of a porous barrier affects the concentration distribution between the canyons. The results show that the concentration spreads vertically along wall A, initiating air circulation inside the canyon.

The presence of a perpendicular box in front of parallel boxes affects the distribution of concentration between buildings. Taking into account porous trees, numerical modeling was performed. For this, the street's size, the linear source's location, and the pollutant's speed also remain unchanged. The full size and boundary data are shown in Figure 8. In this case, the concentration of contaminants was left the same as in the Salim test problem (Salim et al., 2011b).

The size of the street, the location of the linear source, and the speed of the pollutant also remain unchanged. As well as a test problem, local grid thickening was used to optimize calculations in certain areas, reducing the total number of cells and optimizing the computational grid.

As a result, this area's total number of elements was 6,856,346, and the number of nodes was 1,203,946. It is worth noting that the increase in the number of elements is due to a perpendicular block, which affects the computational grid's structure, as shown in Figure 8.

Box A perpendicular box in front of the parallel sides significantly affects concentration levels. The concentration distribution profile is illustrated in Figure 9. Near wall A, at y/H = 0, the molar concentration of Sf_6 decreases to 0.4. However, no significant changes are observed at wall A, where y/H = 3.79.

In contrast, at wall A with y/H = 1.26, a sharp increase in pollution concentration is noted, rising from 0 to 0.4. Thus, it can be explained that the presence of a perpendicular box changes the velocity flow and affects the spread of concentricity between buildings. It is worth noting that near the wall, at y/H = 1.26, the concentration decreases significantly less, and y/H = 0 and y/H = 3.79, a decrease in concentration can be seen only in height.

DISCUSSION

The results of numerical modeling clearly demonstrated that the presence of a perpendicular

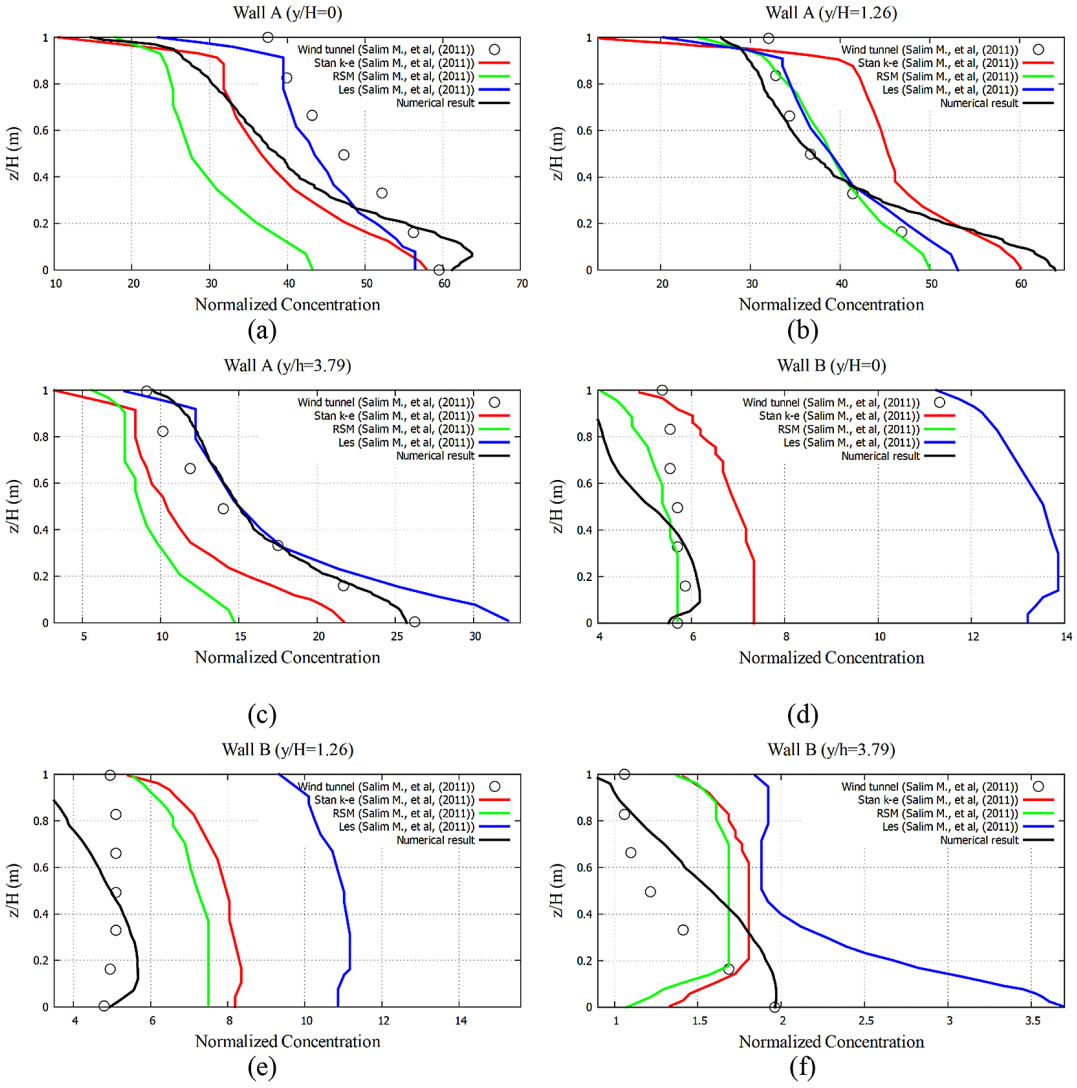

Figure 5. Concentration Sf_6 Molar concentration at six different locations for the test task

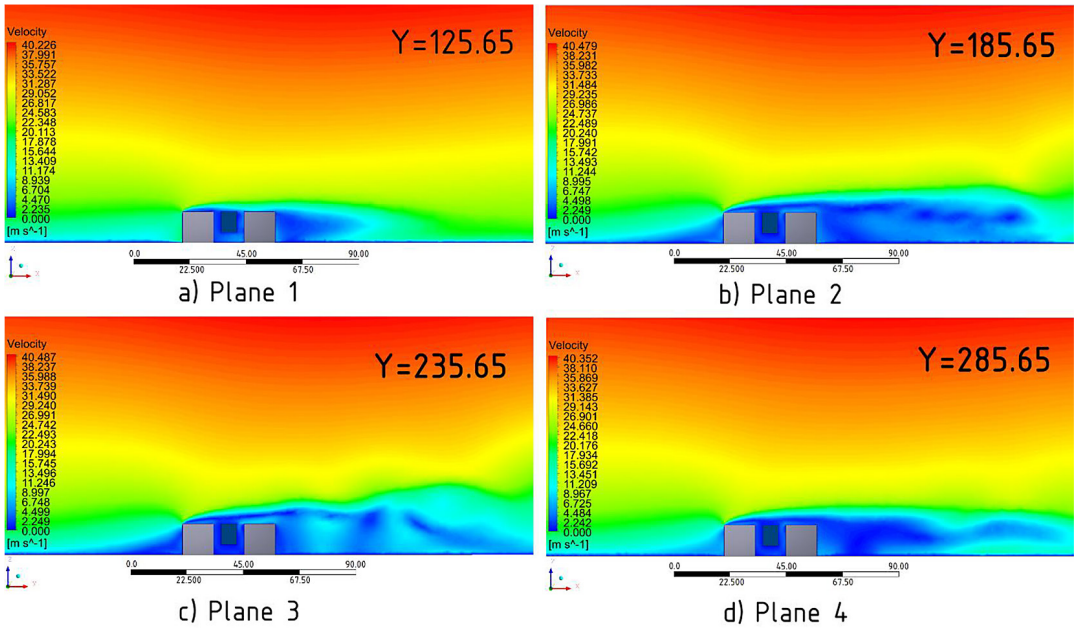

Figure 6. Velocity planes

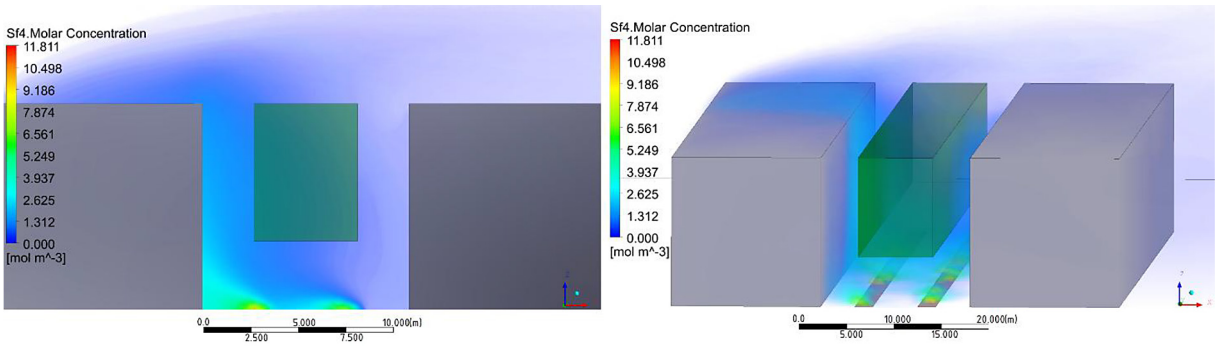

Figure 7. Sf_6 Molar concentration 2D and 3D

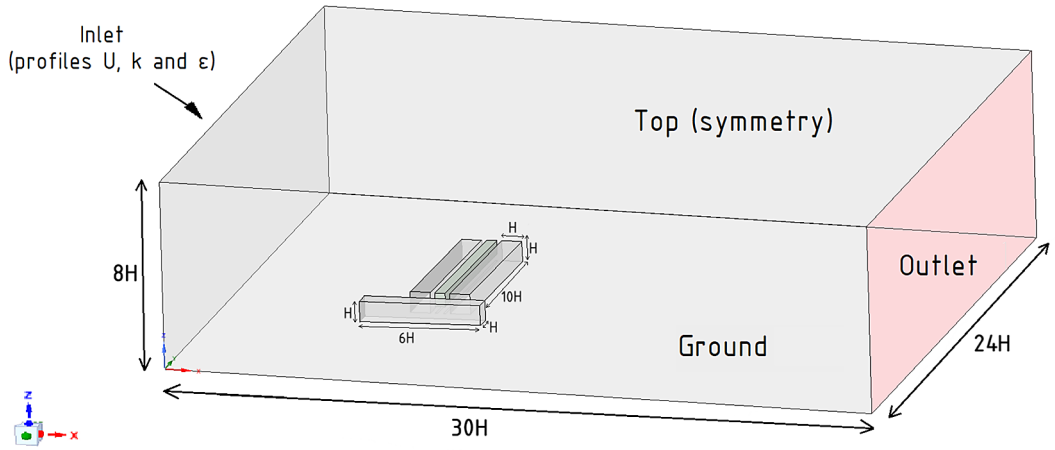

Figure 8. Computational domain model and boundary conditions of new perpendicular box

block within a system of parallel buildings significantly alters the airflow structure and the dispersion of pollutants in a street canyon. The introduction of a porous medium representing tree-like vegetation further modifies flow velocities and redistributes vortex structures. Our results are consistent with experimental data obtained for similar configurations (Salim et al., 2011a) and clearly show that even minor morphological changes in urban layouts can substantially affect ventilation efficiency and pollutant concentrations. Wang et al. (2020) and Bździuch et al. (2024) reported that roadside vegetation, treated as porous obstacles, reduces street and canyon ventilation and enhances pollutant accumulation, which is consistent with the elevated mid-height concentrations observed in our study. Using 3D models to compare hedgerows with solid barriers, Lin et al. (2023) found that vegetated hedges can reduce near-wall pollutant levels by about 59% (compared to 45% for a solid wall) due to the generation of counter-rotating vortices that enhance vertical mixing.

However, most of these studies simplified certain geometric aspects: the canyon was modeled as a long two-dimensional street (or a symmetric three-dimensional canyon) lined with trees or hedges. Tang et al. (2023) analyzed tree foliage density in asymmetric canyons, and Qin et al. (2023) studied vehicle-related emissions, but neither considered perpendicular obstacles. Our work extends this body of research by incorporating a perpendicular block, showing that such elements create zones of secondary recirculation under porous conditions and generate localized pollution hotspots that are not accounted for in standard canyon models.

At the same time, several limitations should be acknowledged. The present modeling employed an idealized canyon geometry and a restricted set of boundary conditions, whereas real cities feature more heterogeneous structures, varied topography, and multiple emission sources. Porosity and turbulence parameters were adopted from literature, introducing uncertainties that may affect quantitative predictions. Although the

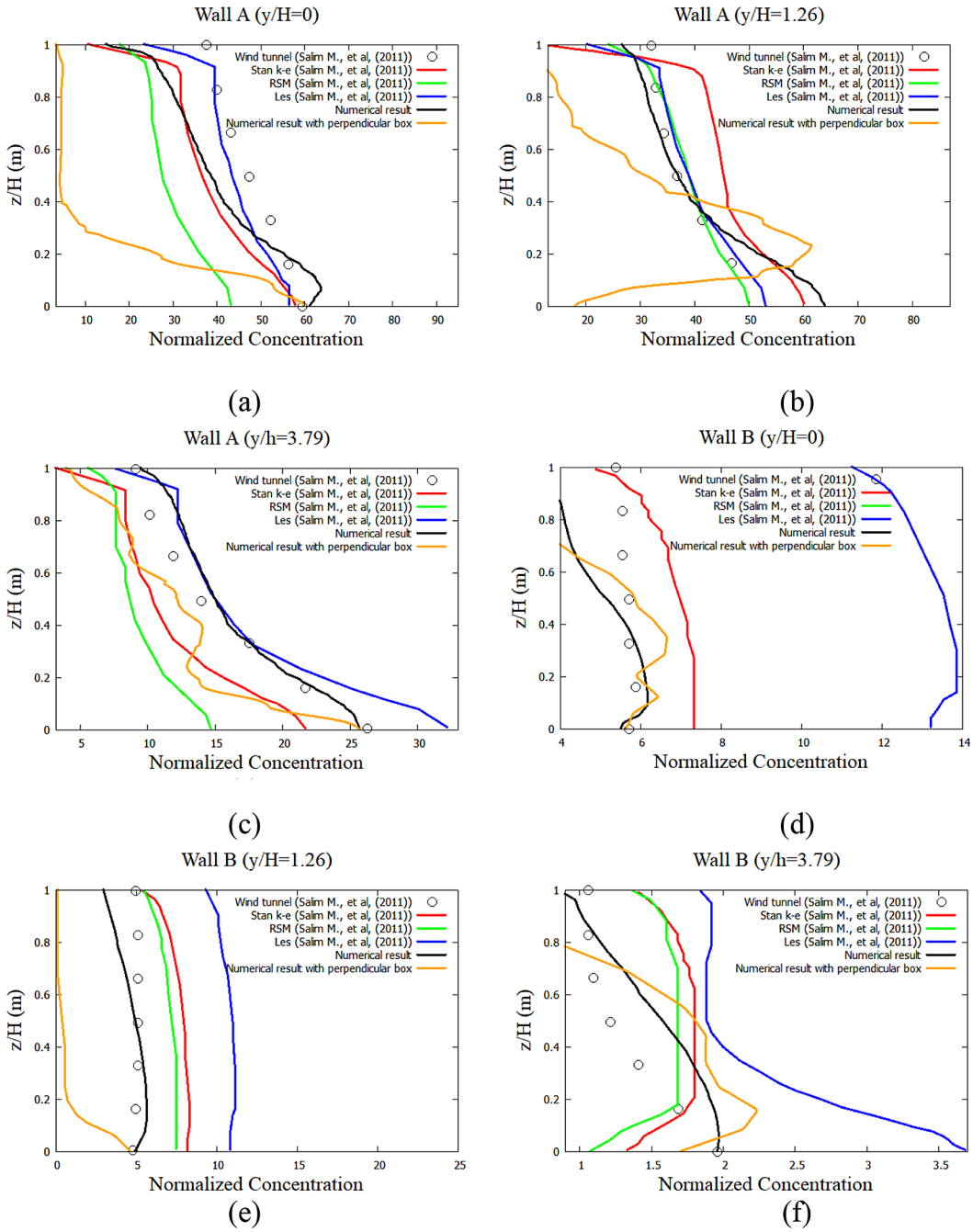

Figure 9. Concentration Sf_6 molar concentration at six different points for new perpendicular

RNG k–ε turbulence model offers computational efficiency, it may not fully capture small-scale vortices that influence pollutant transport in critical regions. Such trade-offs are inherent in CFD studies and highlight the unavoidable balance between accuracy and efficiency.

Despite these limitations, the observed patterns of pollutant fluxes and distributions provide a reliable basis for further research. Future research will extend the simulation to more realistic urban areas, including variable terrain, complex street networks, and seasonal meteorological conditions. Improved turbulence patterns such as LES or hybrid RANS files will be explored to better account for non-stationary characteristics, while broader verification based on field measurements will enhance forecasting capabilities. Ultimately, the results of the study emphasize that even minor design elements, such as perpendicular porous fences, can significantly affect the air quality at the pedestrian level. Awareness of these effects is crucial for urban planning and the

development of effective measures to improve the environment in densely populated areas.

CONCLUSIONS

This study investigates how pollutant concentrations within street canyons are influenced by the presence of porous barriers and urban structural features. Through mathematical modeling, key patterns of pollutant distribution have been identified.

A notable finding is the substantial impact of a perpendicular structure positioned in front of parallel buildings. This combination has a significant impact on air movement and the spread of pollutants in the urban environment. Numerical modeling has shown that such barriers can redistribute airflow, resulting in varying pollutant concentrations across different zones of the canyon.

Pollutants tend to disperse vertically, and an analysis of Wall A reveals that pollutant concentration varies sharply at different heights. Near the height ratio (y/H = 0), the concentration decreases to 0.4, but then there is a sharp increase at (y/H=1.26). In particular, the highest concentration of pollutants occurs in this height ratio, indicating a zone where pollutant levels significantly deviate from the norm. This suggests a challenge to air circulation in this area, which could lead to the accumulation of harmful substances. Identifying this critical area is essential to assess the environmental impact. The data obtained are vital for predicting air pollution under various conditions and developing mitigation strategies.

Future research will focus on extending the model to real urban environments, particularly the city of Almaty, Kazakhstan. This will involve incorporating complex terrain, seasonal meteorological conditions, and multiple emission sources to achieve more realistic predictions. A broader validation with field measurement campaigns is also planned to strengthen the model's predictive capability. In addition, the integration of deep learning techniques for airflow and dispersion modeling will be explored, with the aim of enhancing forecast accuracy and enabling efficient data-driven support for urban air-quality management.

Acknowledgments

This research has been funded by the Committee of Science of the Ministry of Science and Higher Education of the Republic of Kazakhstan (Grant No. BR24992852 "Intelligent models and methods of Smart City digital ecosystem for sustainable development and the citizens' quality of life improvement").

REFERENCES

1. Altaibek, A., Nurtas, M., Zhantayev, Z., Zhumabayev, B., Kumarkhanova, A. (2024). Classifying seismic events linked to solar activity: A retrospective lstm approach using proton density. Atmosphere 15(11), 1290. https://doi.org/10.3390/atmos15111290
2. Assanov, D., Zapasnyi, V., Kerimray, A. (2021). Air quality and industrial emissions in the cities of kazakhstan. Atmosphere 12(3), 314. https://doi.org/10.3390/atmos12030314
3. Badach, J., Dymnicka, M., & Baranowski, A. (2020). Urban vegetation in air quality management: A review and policy framework. Sustainability 12(3), 1258. https://doi.org/10.3390/su12031258
4. Barwise, Y., Kumar, P. (2020). Designing vegetation barriers for urban air pollution abatement: A practical review for appropriate plant species selection. Npj Climate and Atmospheric Science 3(1), 12. https://doi.org/10.1038/s41612-020-0115-3
5. Baydaulet, U., Omarova, P., Merembayev, T., Yedilkhan, A. (2024). Modeling siltation of river channels using the physics-informed neural networks method and numerical simulation. Engineered Science 33, 1296. https://dx.doi.org/10.30919/es1296
6. Blocken, B. (2015). Computational fluid dynamics for urban physics: Importance, scales, pos-sibilities, limitations and ten tips and tricks towards accurate and reliable simulations. Building and Environment 91, 219–245. https://doi.org/10.1016/j.buildenv.2015.02.015
7. Buccolieri, R., Carlo, O.S., Rivas, E., Santiago, J.L. (2021). Urban obstacles influence on street canyon ventilation: a brief review. Environmental Sciences Proceedings 8(1), 11. https://doi.org/10.3390/ecas2021-10350
8. Bździuch, P., Bogacki, M., Oleniacz, R. (2024). Street canyon vegetation-impact on the disper-sion of air pollutant emissions from road traffic. Sustainability 16(23), 10700. https://doi.org/10.3390/su162310700
9. Deng, W., Yang, T., Tang, L., Tang, Y.-T. (2018). Barriers and policy recommendations for developing

green buildings from local government perspective: a case study of Ningbo China. Intelligent Buildings International 10(2), 61–77. https://doi.org/10.1080/17508975.2016.1248342

10. Jeong, N.-R., Han, S.-W., Ko, B. (2023). Effects of green network management of urban street trees on airborne particulate matter (PM2.5) concentration. International Journal of Environmental Research and Public Health 20(3), 2507. https://doi.org/10.3390/ijerph20032507
11. Kalesh, D., Merembayev, T., Omirbekov, S., Amanbek, Y. (2025a). Application of physics-informed neural networks for two-phase flow model with variable diffusion and experimental validation. Results in Engineering, 105439. https://doi.org/10.1016/j.rineng.2025.105439
12. Kalesh, D., Merembayev, T., Omirbekov, S., Amanbek, Y. (2025b). Physics Informed Kolmogo-rov-Arnold Network for Two-Phase Flow Model with Experimental Data. In: International Conference on Computational Science and Its Applications. 447–460. Cham: Springer Nature Switzerland. https://doi.org/10.1007/978-3-031-97596-7_30
13. Kerimray, A., Assanov, D., Kenessov, B., Karaca, F. (2020a). Trends and health impacts of major urban air pollutants in Kazakhstan. Journal of the Air & Waste Management Association 70(11), 1148–1164. https://doi.org/10.1080/10962247.2020.1813837
14. Kerimray, A., Baimatova, N., Ibragimova, O.P., Bukenov, B., Kenessov, B., Plotit syn, P., Karaca, F. (2020b). Assessing air quality changes in large cities during Covid-19 lockdowns: The impacts of traffic-free urban conditions in Almaty, Kazakhstan. Science of the Total Environment 730, 139179. https://doi.org/10.1016/J.SCITOTENV.2020.139179
15. Kerimray, A., Azbanbayev, E., Kenessov, B., Plotitsyn, P., Alimbayeva, D., Karaca, F. (2020c). Spatiotemporal variations and contributing factors of air pollutants in Almaty, Kazakhstan. Aerosol and Air Quality Research 20(6), 1340–1352. https://doi.org/10.4209/aaqr.2019.09.0464
16. Kim, Y.-U., Lee, S.-B., Kim, C.H., Lee, S., Kwak, K.-H. (2025). Aerodynamic and dry deposition effects of roadside trees on nox concentration changes on roadways and sidewalks. Atmosphere 16(3), 344. https://doi.org/10.3390/atmos16030344
17. Li, D., Liu, J., Zhao, Y. (2022). Prediction of multi-site PM2.5 concentrations in beijing using CNN-bi lstm with CBAM. Atmosphere 13(10), 1719. https://doi.org/10.3390/atmos13101719
18. Li, Q., Liang, J., Wang, Q., Chen, Y., Yang, H., Ling, H., Luo, Z., Hang, J. (2022). Numerical inves-tigations of urban pollutant dispersion and building intake frac tion with various 3d building configurations and tree plantings. International Journal of Environmental Research and Public Health 19(6), 3524. https://doi.org/10.3390/ijerph19063524
19. Lin, C., Ooka, R., Kikumoto, H., Flageul, C., Kim, Y., Wang, Y., Sartelet, K. (2023). Large-eddy simulations on pollutant reduction effects of hedge and solid barriers in an idealized street canyon. http://doi.org/10.2139/ssrn.4390474
20. Liu, J., Zheng, B. (2023). A simulation study on the influence of street tree configuration on fine particulate matter (PM2.5) concentration in street canyons. Forests 14(8), 1550 https://doi.org/10.3390/f14081550
21. Mohammadi, M., Calautit, J. (2021). Impact of ventilation strategy on the transmission of outdoor pollutants into indoor environment using cfd. Sustainability 13(18), 10343. https://doi.org/10.3390/SU131810343
22. Mutlu, M. (2020). Numerical investigation of indoor air quality in a floor heated room with different air change rates. Building Simulation, 13, 1063–1075. https://doi.org/10.1007/s12273-020-0683-5
23. Oke, T.R. (2002). Boundary Layer Climates. Routledge, 3 Park Square, Milton Park, Oxford-shire.
24. Omarova, P., Amirgaliyev, Y., Kozbakova, A., Ataniyazova, A. (2023). Application of physics-informed neural networks to river silting simulation. Applied Sciences 13(21), 11983. https://doi.org/10.3390/app132111983
25. Pantusheva, M., Mitkov, R., Hristov, P.O., Petrova-Antonova, D. (2022). Air pollu tion disper-sion modelling in urban environment using cfd: a systematic review. Atmosphere 13(10), 1640. https://doi.org/10.3390/atmos13101640
26. Qin, P., Ricci, A., Blocken, B. (2023). CFD simulation of pollutant dispersion in a street canyon: Impact of idealized and realistic sources. In E3S Web of Conferences. http://doi.org/10.1051/e3sconf/202339602042
27. Raissi, M., Perdikaris, P., Karniadakis, G.E. (2019). Physics-informed neural networks: A deep learning framework for solving forward and inverse problems involving nonlinear partial differential equations. Journal of Computational Physics 378, 686–707. https://doi.org/10.1016/j.jcp.2018.10.045
28. Salim, S.M., Cheah, S.C., Chan, A. (2011a). Numerical simulation of dispersion in urban street canyons with avenue-like tree plantings: comparison between rans and les. Building and Environment 46(9), 1735–1746. https://doi.org/10.1016/j.buildenv.2011.01.032
29. Salim, S.M., Buccolieri, R., Chan, A., Di Sabatino, S. (2011b). Numerical simulation of atmos-pheric pollutant dispersion in an urban street canyon: Comparison between rans and les. Journal of Wind Engineering and Industrial Aerodynamics 99(2–3), 103–113.https://doi.org/10.1016/j.jweia.2010.12.002

30. Santiago, J.-L., Buccolieri, R., Rivas, E., Calvete-Sogo, H., Sanchez, B., Martilli, A., Alonso, R., Elustondo, D., Santamaria, J.M., Martin, F. (2019). Cfd modelling of vegetation barrier effects on the reduction of traffic-related pollutant concentration in an avenue of Pamplona, Spain. Sustainable Cities and Society 48, 101559. https://doi.org/10.1016/j.scs.2019.101559
31. Sha, C., Wang, X., Lin, Y., Fan, Y., Chen, X., Hang, J. (2018). The impact of urban open space and 'lift-up'building design on building intake fraction and daily pollutant exposure in ideal-ized urban models. Science of the Total Environment 633, 1314–1328. https://doi.org/10.1016/j.scitotenv.2018.03.194
32. Sin, C.H., Cui, P.-Y., Jon, K.S., Luo, Y., Shen, J.-W., Huang, Y.-d. (2023). Evaluation on ventilation and traffic pollutant dispersion in asymmetric street canyons with void decks. Air Quality, Atmosphere & Health 16(4), 817–839. https://doi.org/10.1007/s11869-023-01314-3
33. Tang, Y. F., Wen, Y. B., Chen, H., Tan, Z. C., Yao, Y. H., Zhao, F. Y. (2023). Airflow mitigation and pollutant purification in an idealized urban street canyon with wind driven natural ventila-tion: co-operating and opposing effects of roadside tree plantings and non-uniform building heights. Sustainable Cities and Society, 92, 104483. http://doi.org/10.2139/ssrn.4330197
34. Tominaga, Y. (2015). Flow around a high-rise building using steady and unsteady rans cfd: Effect of large-scale fluctuations on the velocity statistics. Journal of Wind Engineering and Industrial Aerodynamics 142, 93–103. https://doi.org/10.1016/j.jweia.2015.03.013
35. Wang, L., Su, J., Gu, Z., Shui, Q. (2020). Effect of street canyon shape and tree layout on pollu-tant diffusion under real tree model. Sustainability 12(5), 2105. https://doi.org/10.3390/su12052105
36. Weaver, D.S., Miskovic, S. (2021). A study of rans turbulence models in fully turbulent jets: a perspective for cfd-dem simulations. Fluids 6(8), 271. https://doi.org/10.3390/fluids6080271
37. Wijesooriya, K., Mohotti, D., Lee, C.-K., Mendis, P. (2023). A technical review of com putation-al fluid dynamics (cfd) applications on wind design of tall buildings and structures: Past, present and future. Journal of Building Engineering 74, 106828. https://doi.org/10.1016/J.JOBE.2023.106828
38. Yakhot, V., Orszag, S.A. (1986). Renormalization group analysis of turbulence. Basic theory. Journal of scientific computing 1(1), 3–51. https://doi.org/10.1007/BF01061452
39. Yang T., D.J.C.-C. (2020). Natural ventilation in built environment. Sustainable Built Environments, 431–464. https://doi.org/10.1007/978-1-4939-2493-6_488-3
40. Yang, T.: A whole-system approach to high-performance green buildings. (2017). Intelligent Buildings International 9(3), 177–178. https://doi.org/10.1080/17508975.2017.1327237
41. Yedilkhan, M., Berdyshev, A., Galiyev, M., Merembayev, T. (2025). Air quality prediction based on the lstm with attention using meteorological data in urban area in Kazakhstan. Journal of Problems in Computer Science and Information Technologies, 3(1), 3–12. https://doi.org/10.26577/jpcsit20253101
42. Zhang, Q., Wu, S., Wang, X., Sun, B., Liu, H. (2020). A pm2.5 concentration prediction model based on multi-task deep learning for intensive air quality monitoring stations. Journal of Cleaner Production. 275, 122722. https://doi.org/10.1016/j.jclepro.2020.122722
43. Zhang, Y., Gu, Z., & Yu, C.W. (2020). Impact factors on airflow and pollutant dispersion in ur-ban street canyons and comprehensive simulations: A review. Current Pollution Reports 6, 425–439. https://doi.org/10.1007/s40726-020-00166-0
44. Zheng, X., Montazeri, H., Blocken, B. (2021). Large-eddy simulation of pollutant dis persion in generic urban street canyons: Guidelines for domain size. Journal of Wind Engineering and Industrial Aerodynamics 211, 104527. https://doi.org/10.1016/j.jweia.2021.104527